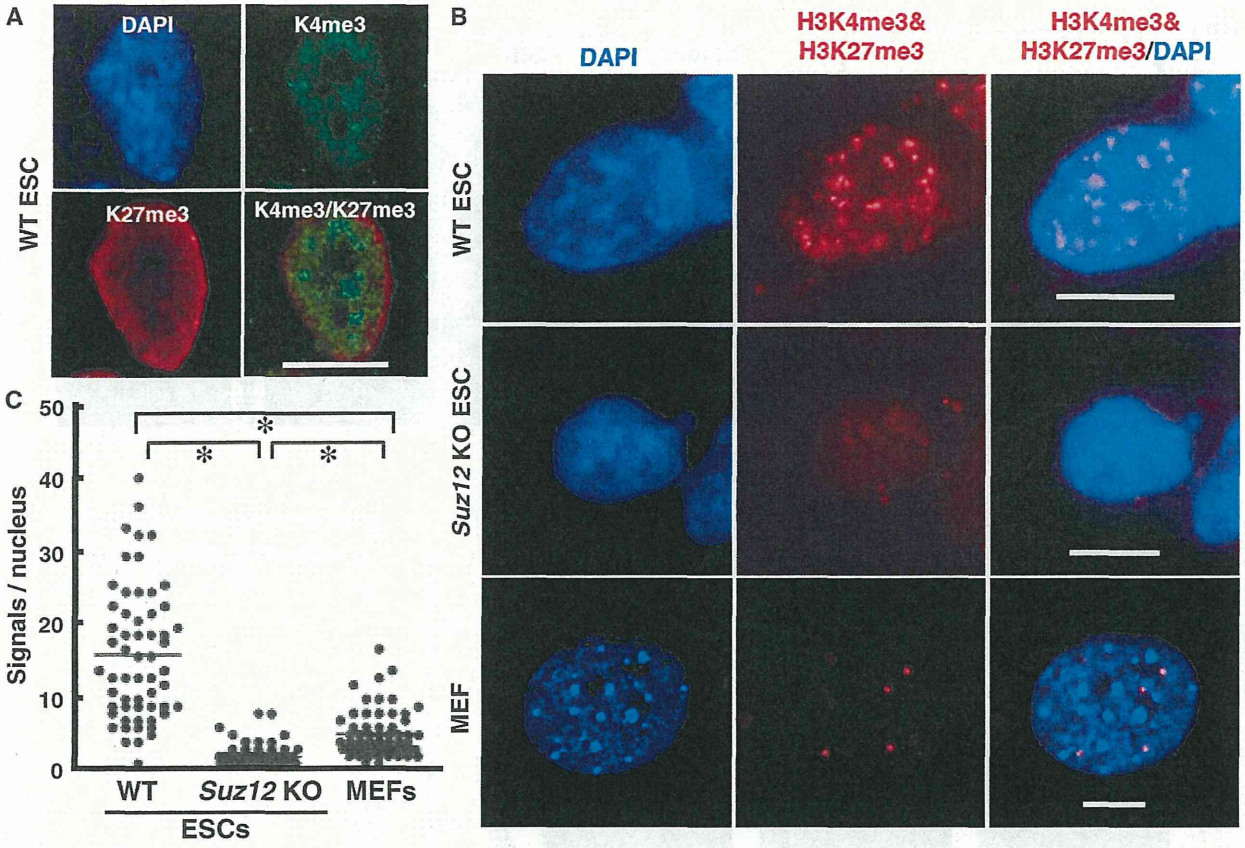

Figure 2. Application of iChmo to visualization of bivalent modification. (**A**) Mouse ESCs were stained by immunofluorescence with antibodies against H3K4me3 and H3K27me3 (scale bar: 10 μm). (**B**) Coexistence of H3K4me3 and H3K27me3 in WT ESCs was detected by iChmo, but hardly in *Suz12* KO ESCs and MEFs (scale bar: 10 μm). (**C**) The mean number of fluorescence spots was significantly larger in WT ESCs (15.2; $n = 58$) than in *Suz12* KO ESCs (0.9; $n = 69$) and MEFs (4.1; $n = 60$) (Mann–Whitney *U*-test; $*P < 0.001$).

human tissue sample, we first screened 11 antibodies that had high specificity applicable to iChmo using cultured cells and identified that a combination of antibodies against H3K9me3 and H4K20me3 could be used for tissues samples (Figure 4A and B). Small dots of H3K9me3 were detected in all the cells of a human colonic tissue, presenting a similar staining pattern to that of cultured cells. Signals of H4K20me3 were also detected, and small dots of H3K9me3 were merged with those of H4K20me3 (Figure 4B). By iChmo, fluorescence spots were observed (Figure 4C) and were localized in the nuclei of cells (Figure 4D). Notably, the appearance of iChmo spots of H3K9me3 and H4K20me3 showed heterogeneity among the cells, and the cells that lacked iChmo spots corresponded to those that had strong DAPI intensity (Figure 4C and Supplementary Figure S4A and B), indicating that the presence of a combination of H3K9me3 and H4K20me3 was dependent on a cell condition, such as the cell cycle. The possibility that fluorescence spots were produced by non-specific binding of PLA probes was excluded by the absence of iChmo spots (Supplementary Figure S4E) using antibodies against H3K9ac and H4K20me3 (Supplementary Figure S4C and D).

DISCUSSION

An imaging method for a combination of epigenetic modifications in close proximity was established and was designated as iChmo. It had the capacity to visualize the combinations at the single cell level and thus was able to analyze heterogeneous samples, such as a cell line consisting of cells at various differentiation stages and tissue samples.

The application of iChmo to ESCs at their differentiation revealed that the epigenetic layer of differentiation takes place in a highly concerted manner before the phenotypic layer of differentiation. Previous reports showed that gene expression changes at several genes occur in parallel with histone modification changes during ESC differentiation (21,22). In addition, it is reported that, at *Hoxa1* and *Sox21*, development-related genes marked with bivalent modification, H3K27me3 levels decreased before gene activation at the early stage of ESC differentiation (23,24). However, up to now, it has been impossible to analyze to what degree such histone modification changes are concerted among cells during ESC differentiation, and the use of iChmo revealed highly concerted change. Also, taking advantage of its

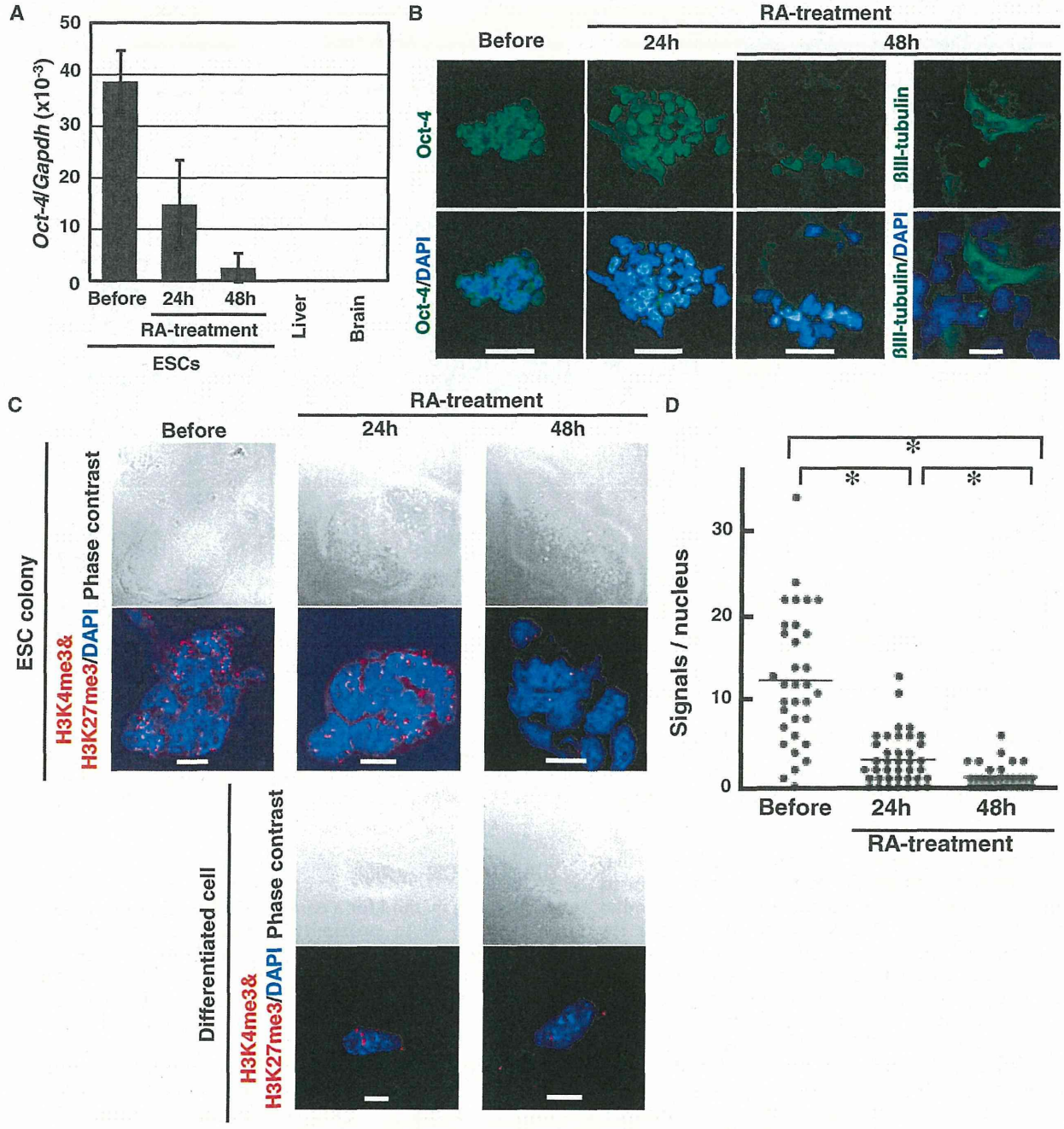

Figure 3. Visualization of epigenetic and phenotypic layers of differentiation in an early stage of ESC differentiation. (**A**) Differentiation of ESCs was induced by treatment of all-trans RA, and *Oct-4* mRNA expression was measured before, and 24 and 48 h after the RA treatment. The expression levels in the mouse liver and brain are shown as those in *Oct-4*-negative tissues. Values show mean + SD of three experiments. (**B**) Expression of Oct-4 and ßIII-tubulin proteins was analyzed in ESCs before, and 24 and 48 h after the RA treatment by immunofluorescence (scale bar: 20 μm). (**C**) Images of phase contrast and iChmo for the bivalent modification in ESC colonies before, and 24 and 48 h after the RA treatment (upper panel), and differentiated neuron-like cells at 24 and 48 h (lower panel). Regardless of the phenotypic differentiation statuses, the bivalent modification was absent both at 24 and 48 h, supporting highly concerted regulation of epigenetic changes. Scale bar represents 10 μm. (**D**) The number of fluorescence spots was counted in ESCs before ($n = 33$), and 24 ($n = 37$) and 48 ($n = 38$) h after the RA treatment (Mann–Whitney *U*-test; $*P < 0.001$). Although the decrease of Oct-4 expression and increase of ßIII-tubulin were highly variable among the ESCs treated with RA, the decrease of the bivalent modification was highly coordinated.

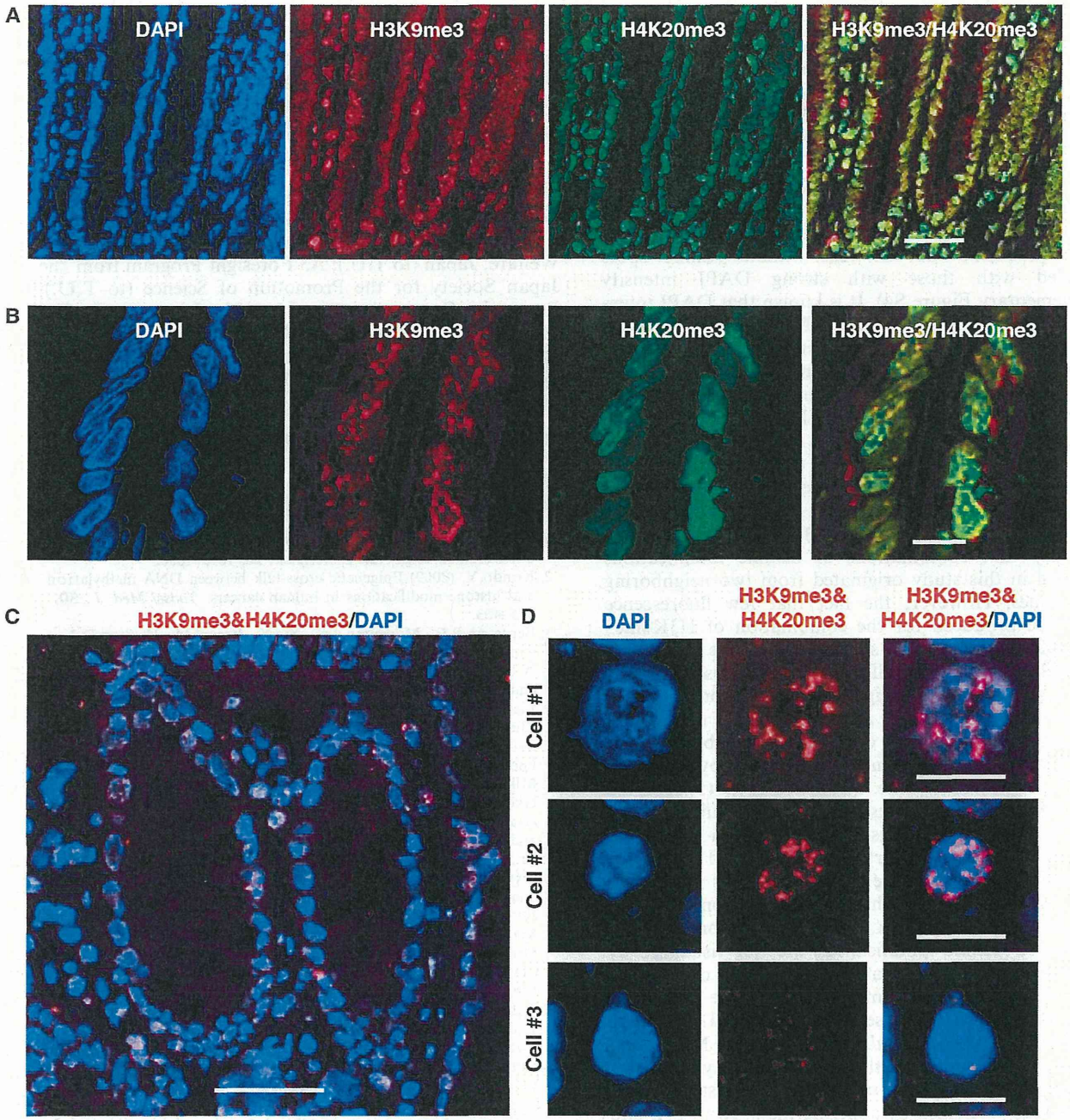

Figure 4. Application of iChmo to the analysis of human colonic tissue. (**A**) Human colonic tissues were stained by immunofluorescence with antibodies against H3K9me3 and H4K20me3 (scale bar: 50 μm). Colocalization of H3K9me3/ H4K20me3 was observed in the cells of colonic tissue. (**B**) High-magnification images of (A) (scale bar: 10 μm). (**C**) Coexistence of H3K9me3 and H4K20me3 was visualized in the nuclei of cells as fluorescence spots (scale bar: 50 μm). (**D**) High-magnification images of (C) (scale bar: 10 μm). The cells with iChmo spots (Cell #1 and #2) coincided with the cells having weak DAPI intensity, and the cells without iChmo spots (Cell #3) showed strong DAPI intensity.

applicability to a heterogeneous cell population and the role of bivalent modification in 'stemness', iChmo might be able to evaluate the level of cell reprogramming and the quality of iPS cells (25).

iChmo is also used for analysis of tissue sections. Although we analyzed only a limited number of combinations of histone modifications for now owing to availability of specific antibodies, analysis of tissue samples is expected to produce rich information, such as localization of tissue stem cells. Indeed, Lien *et al.* (4) clearly showed that the combination of H3K4me3 and H3K79me2 was specifically found in quiescent hair follicle

stem cells by ChIP-sequencing. We can expect that, by using iChmo, the presence of such combination of histone modifications can be demonstrated in a small amount of cells of histological sections. Also, aberrant expression of histone modifiers is now becoming evident in human disorders, especially in cancers (26), and iChmo might clarify which aberrant combinations are present, even if the fraction of cells with such aberrant combinations is small.

Analysis of human colonic tissue samples revealed the presence of heterogeneity of iChmo spots of H3K9me3 and H4K20me3, and the cells without iChmo spots coincided with those with strong DAPI intensity (Supplementary Figure S4). It is known that DAPI intensity is affected by DNA content, reflecting the phase of the cell cycle. In addition, considering that the levels of H3K9me3 and H4K20me3 dynamically change during the cell cycle (27), we can speculate that the heterogeneity of iChmo spots of H3K9me3 and H4K20me3 reflects the difference of the phases of the cell cycle.

The maximum distance between the primary antibodies recognized by two PLA probes has been estimated to be ~30 nm (14), which is longer than the minimum distance between two nucleosomes (~15 nm). Thus, there remains a possibility that combinations of histone modifications visualized in this study originated from two neighboring nucleosomes. However, the fact that few fluorescence spots were produced for the combination of H3K4me3 and H3K27me3 in MEFs supported that the signals are produced from two modifications at a close distance, theoretically within two neighboring nucleosomes.

iChmo showed a large number of spots of bivalent modification in ESCs, but only a small number of spots in MEFs, which was in line with a report by Bernstein *et al.* (3). At the same time, Mikkelsen *et al.* (5) reported that a half of bivalent marks in mouse ESCs still remained in MEFs. The apparent discrepancy between the iChmo data and the previous report can be accounted for by two possibilities; (i) because one iChmo spot does not always reflect one combination of histone modifications owing to the principle of *in situ* PLA (14), and all regions with co-existence of histone modifications are not visualized by this method, and (ii) because the number of bivalent marks is different according to the culture period of MEFs. In this study, we used MEFs cultured at passage five, whereas Mikkelsen *et al.* (5) used primary MEFs, and the authors also suggested the latter possibility.

To summarize, a specific combination of histone modifications was visualized by applying the *in situ* PLA, and the method was capable of analyzing heterogeneous cell population and tissue samples. Application of the method has the potential to uncover previously unknown biological and pathological significances of combinations of histone modifications.

SUPPLEMENTARY DATA

Supplementary Data are available at NAR Online: Supplementary Table 1, Supplementary Figures 1–4, Supplementary Methods and Supplementary Reference [28].

ACKNOWLEDGEMENTS

The authors thank Dr K. Shiota (The University of Tokyo) for providing them MEFs, and Drs T. Imai and N. Uchiya, and National Cancer Center Research Core Facility for the preparation of human tissues sections.

FUNDING

Grant-in-Aid for the Third-Term Comprehensive Cancer Control Strategy from the Ministry of Health, Labour and Welfare, Japan (to T.U.); A3 Foresight Program from the Japan Society for the Promotion of Science (to T.U.); Research Grants in the Natural Sciences of The Mitsubishi Foundation (to T.U. and N.H.). Funding for open access charge: Third-Term Comprehensive Cancer Control Strategy from the Ministry of Health, Labour and Welfare, Japan.

Conflict of interest statement. None declared.

REFERENCES

1. Meissner,A. (2010) Epigenetic modifications in pluripotent and differentiated cells. *Nat. Biotechnol.*, **28**, 1079–1088.
2. Kondo,Y. (2009) Epigenetic cross-talk between DNA methylation and histone modifications in human cancers. *Yonsei Med. J.*, **50**, 455–463.
3. Bernstein,B.E., Mikkelsen,T.S., Xie,X., Kamal,M., Huebert,D.J., Cuff,J., Fry,B., Meissner,A., Wernig,M., Plath,K. *et al.* (2006) A bivalent chromatin structure marks key developmental genes in embryonic stem cells. *Cell*, **125**, 315–326.
4. Lien,W.H., Guo,X., Polak,L., Lawton,L.N., Young,R.A., Zheng,D. and Fuchs,E. (2011) Genome-wide maps of histone modifications unwind in vivo chromatin states of the hair follicle lineage. *Cell Stem Cell*, **9**, 219–232.
5. Mikkelsen,T.S., Ku,M., Jaffe,D.B., Issac,B., Lieberman,E., Giannoukos,G., Alvarez,P., Brockman,W., Kim,T.K., Koche,R.P. *et al.* (2007) Genome-wide maps of chromatin state in pluripotent and lineage-committed cells. *Nature*, **448**, 553–560.
6. Rada-Iglesias,A., Bajpai,R., Swigut,T., Brugmann,S.A., Flynn,R.A. and Wysocka,J. (2011) A unique chromatin signature uncovers early developmental enhancers in humans. *Nature*, **470**, 279–283.
7. Xiao,S., Xie,D., Cao,X., Yu,P., Xing,X., Chen,C.C., Musselman,M., Xie,M., West,F.D., Lewin,H.A. *et al.* (2012) Comparative epigenomic annotation of regulatory DNA. *Cell*, **149**, 1381–1392.
8. Ruthenburg,A.J., Li,H., Milne,T.A., Dewell,S., McGinty,R.K., Yuen,M., Ueberheide,B., Dou,Y., Muir,T.W., Patel,D.J. *et al.* (2011) Recognition of a mononucleosomal histone modification pattern by BPTF via multivalent interactions. *Cell*, **145**, 692–706.
9. Vastenhouw,N.L., Zhang,Y., Woods,I.G., Imam,F., Regev,A., Liu,X.S., Rinn,J. and Schier,A.F. (2010) Chromatin signature of embryonic pluripotency is established during genome activation. *Nature*, **464**, 922–926.
10. Roh,T.Y., Cuddapah,S., Cui,K. and Zhao,K. (2006) The genomic landscape of histone modifications in human T cells. *Proc. Natl Acad. Sci. USA*, **103**, 15782–15787.
11. Tsai,W.W., Wang,Z., Yiu,T.T., Akdemir,K.C., Xia,W., Winter,S., Tsai,C.Y., Shi,X., Schwarzer,D., Plunkett,W. *et al.* (2010) TRIM24 links a non-canonical histone signature to breast cancer. *Nature*, **468**, 927–932.
12. Geisberg,J.V. and Struhl,K. (2004) Quantitative sequential chromatin immunoprecipitation, a method for analyzing co-occupancy of proteins at genomic regions in vivo. *Nucleic Acids Res.*, **32**, e151.
13. Voigt,P., LeRoy,G., Drury,W.J. 3rd, Zee,B.M., Son,J., Beck,D.B., Young,N.L., Garcia,B.A. and Reinberg,D. (2012) Asymmetrically modified nucleosomes. *Cell*, **151**, 181–193.

14. Soderberg,O., Gullberg,M., Jarvius,M., Ridderstrale,K., Leuchowius,K.J., Jarvius,J., Wester,K., Hydbring,P., Bahram,F., Larsson,L.G. *et al.* (2006) Direct observation of individual endogenous protein complexes in situ by proximity ligation. *Nat. Methods*, **3**, 995–1000.
15. Pasini,D., Bracken,A.P., Hansen,J.B., Capillo,M. and Helin,K. (2007) The polycomb group protein Suz12 is required for embryonic stem cell differentiation. *Mol. Cell. Biol.*, **27**, 3769–3779.
16. Perez-Burgos,L., Peters,A.H., Opravil,S., Kauer,M., Mechtler,K. and Jenuwein,T. (2004) Generation and characterization of methyl-lysine histone antibodies. *Methods Enzymol.*, **376**, 234–254.
17. Kimura,H., Hayashi-Takanaka,Y., Goto,Y., Takizawa,N. and Nozaki,N. (2008) The organization of histone H3 modifications as revealed by a panel of specific monoclonal antibodies. *Cell Struct. Funct.*, **33**, 61–73.
18. Kim,T.H., Barrera,L.O., Qu,C., Van Calcar,S., Trinklein,N.D., Cooper,S.J., Luna,R.M., Glass,C.K., Rosenfeld,M.G., Myers,R.M. *et al.* (2005) Direct isolation and identification of promoters in the human genome. *Genome Res.*, **15**, 830–839.
19. Ku,M., Koche,R.P., Rheinbay,E., Mendenhall,E.M., Endoh,M., Mikkelsen,T.S., Presser,A., Nusbaum,C., Xie,X., Chi,A.S. *et al.* (2008) Genomewide analysis of PRC1 and PRC2 occupancy identifies two classes of bivalent domains. *PLoS Genet.*, **4**, e1000242.
20. Pasini,D., Bracken,A.P., Jensen,M.R., Lazzerini Denchi,E. and Helin,K. (2004) Suz12 is essential for mouse development and for EZH2 histone methyltransferase activity. *EMBO J.*, **23**, 4061–4071.
21. Lee,E.R., Murdoch,F.E. and Fritsch,M.K. (2007) High histone acetylation and decreased polycomb repressive complex 2 member levels regulate gene specific transcriptional changes during early embryonic stem cell differentiation induced by retinoic acid. *Stem Cells*, **25**, 2191–2199.
22. Feldman,N., Gerson,A., Fang,J., Li,E., Zhang,Y., Shinkai,Y., Cedar,H. and Bergman,Y. (2006) G9a-mediated irreversible epigenetic inactivation of Oct-3/4 during early embryogenesis. *Nat. Cell Biol.*, **8**, 188–194.
23. Chakravarthy,H., Ormsbee,B.D., Mallanna,S.K. and Rizzino,A. (2011) Rapid activation of the bivalent gene Sox21 requires displacement of multiple layers of gene-silencing machinery. *FASEB J.*, **25**, 206–218.
24. Lee,T.I., Jenner,R.G., Boyer,L.A., Guenther,M.G., Levine,S.S., Kumar,R.M., Chevalier,B., Johnstone,S.E., Cole,M.F., Isono,K. *et al.* (2006) Control of developmental regulators by Polycomb in human embryonic stem cells. *Cell*, **125**, 301–313.
25. Hanna,J.H., Saha,K. and Jaenisch,R. (2010) Pluripotency and cellular reprogramming: facts, hypotheses, unresolved issues. *Cell*, **143**, 508–525.
26. Chi,P., Allis,C.D. and Wang,G.G. (2010) Covalent histone modifications–miswritten, misinterpreted and mis-erased in human cancers. *Nat. Rev. Cancer*, **10**, 457–469.
27. Black,J.C., Van Rechem,C. and Whetstine,J.R. (2012) Histone lysine methylation dynamics: establishment, regulation, and biological impact. *Mol. Cell*, **48**, 491–507.
28. Takeshima,H., Yamashita,S., Shimazu,T., Niwa,T. and Ushijima,T. (2009) The presence of RNA polymerase II, active or stalled, predicts epigenetic fate of promoter CpG islands. *Genome Res.*, **19**, 1974–1982.

JJCO Japanese Journal of Clinical Oncology

Jpn J Clin Oncol 2013;43(6)641–645
doi:10.1093/jjco/hyt058
Advance Access Publication 25 April 2013

Stronger Prognostic Power of the CpG Island Methylator Phenotype than Methylation of Individual Genes in Neuroblastomas

Kiyoshi Asada[1], Naoko Watanabe[1], Yohko Nakamura[2], Miki Ohira[3], Frank Westermann[4], Manfred Schwab[4], Akira Nakagawara[2] and Toshikazu Ushijima[1,*]

[1]Division of Epigenomics, National Cancer Center Research Institute, Tokyo, [2]Division of Biochemistry and Innovative Cancer Therapeutics, Chiba Cancer Center Research Institute, [3]Laboratory of Cancer Genomics, Chiba Cancer Center Research Institute, Chiba, Japan and [4]Division of Tumor Genetics, German Cancer Research Center, Heidelberg, Germany

*For reprints and all correspondence: Toshikazu Ushijima, Division of Epigenomics, National Cancer Center Research Institute, 5-1-1 Tsukiji, Chuo-ku, Tokyo 104-0045, Japan. E-mail: tushijim@ncc.go.jp

Received January 14, 2013; accepted March 30, 2013

Objective: The CpG island methylator phenotype is strongly associated with poor survival in neuroblastomas. Neuroblastomas with the CpG island methylator phenotype include almost all neuroblastomas with *MYCN* amplification, and, even among neuroblastomas without *MYCN* amplification, have worse prognosis. At the same time, methylation of individual tumor-suppressor genes is also reported to be associated with poor survival. The purpose of this study was to compare the prognostic power of the CpG island methylator phenotype with that of methylation of individual genes.

Methods: Methylation-specific polymerase chain reaction was performed for five individual genes (*CASP8*, *EMP3*, *HOXA9*, *NR1I2* and *CD44*) in 140 Japanese and 152 German neuroblastomas. Kaplan–Meier analysis and log-rank tests were conducted to compare the survival between groups defined by methylation status.

Results: Among the five individual genes, only *CASP8* methylation had a significant association with poor overall survival both in Japanese (hazard ratio = 3.1; 95% confidence interval = 1.5–6.4; $P = 0.002$) and German (hazard ratio = 4.8; 95% confidence interval = 2.1–11; $P = 0.0002$) neuroblastomas. *HOXA9* and *NR1I2* methylation were associated with poor survival only in German neuroblastomas. On the other hand, the CpG island methylator phenotype had a strong and consistent association in Japanese (hazard ratio = 22; 95% confidence interval = 5.3–93; $P = 1.5 \times 10^{-5}$) and German (hazard ratio = 9.5; 95% confidence interval = 3.2–28; $P = 4.7 \times 10^{-5}$) neuroblastomas.

Conclusion: The CpG island methylator phenotype is likely to have stronger prognostic power than methylation of individual genes in neuroblastomas.

Key words: neuroblastoma – methylation – CIMP – poor survival

INTRODUCTION

Neuroblastoma (NBL) is the most frequent extracranial pediatric tumor (1). The CpG island methylator phenotype (CIMP), methylation of multiple CpG islands (CGIs), was associated with poor survival with a hazard ratio (HR) of 22 [95% confidence interval (95% CI) = 5.3–93] in Japanese and 9.5 (95% CI = 3.2–28) in German NBLs, respectively (2,3). The prognostic significance of CIMP was further confirmed in Italian NBLs by a pyrosequencing assay (4). Notably, NBLs with CIMP included almost all NBLs with *MYCN* amplification (37/38 in Japanese and 23/23 in German NBLs), the strongest current prognostic marker (5–7). Even among NBLs without

MYCN amplification, CIMP was a significant and strong prognostic marker with an HR of 12 (95% CI = 2.6–59) in Japanese and 4.5 (95% CI = 1.3–16) in German NBLs.

CIMP is sensitively detected by methylation of marker CGIs, such as CGIs in gene bodies of the *PCDHB* gene family in NBLs. It is known that methylation of CGIs outside promoter regions (non-promoter CGIs) is not associated with loss of expression, and such non-promoter CGIs are more susceptible to methylation induction than promoter CGIs (8). As a model of the close association between methylation of non-promoter CGIs and poor survival, it was considered that CIMP consistently leads to methylation of non-promoter CGIs, such as CGIs of the *PCDHB* gene family in NBLs, and also to methylation of various promoter CGIs with low incidences, which causes poor survival.

At the same time, methylation of an individual gene has been also shown to be associated with poor survival. For example, methylation of *CASP8* was associated with poor survival with an HR of 5.3 (95% CI = 1.5–18; $P = 0.008$) (9). Methylation of *NR1I2*, *EMP3*, *HOXA9* and *CD44* was associated with poor survival with P values of 0.014, 0.03, 0.04 and 0.049, respectively (9–12). Functionally, *CASP8*, an apoptosis-related gene, has been reported to act as a tumor suppressor, and its loss is required for survival of NBL cells overexpressing *MYC* or *MYCN* (13). *NR1I2* (a nuclear receptor gene) and *EMP3* (a myelin-related gene) have been reported to have growth suppressive activity in NBL cells (10,11). However, the prognostic powers of methylation of these individual genes and of CIMP have never been analyzed in identical sets of NBLs.

In the present study, we aimed to compare the prognostic power of CIMP with that of methylation of individual genes.

PATIENTS AND METHODS

DNA Samples and Analysis of CIMP

The 140 Japanese and 152 German NBLs were identical with those analyzed in our previous studies (2,3). These samples were analyzed at the Division of Epigenomics, National Cancer Center Research Institute under the approval of institutional review boards. The presence of CIMP and *MYCN* amplification were determined as in our previous studies (2,3), and this information was used in the present study.

Sodium Bisulfite Modification and Methylation-specific Polymerase Chain Reaction (PCR)

Fully methylated DNA and fully unmethylated DNA were prepared by methylating genomic DNA with *Sss*I methylase (New England Biolabs, Beverly, MA, USA) and by amplifying genomic DNA with the GenomiPhi amplification system (GE Health Care, Buckinghamshire, UK), respectively. Bisulfite modification was performed using 1 μg of *Bam*HI-digested genomic DNA as previously described (14), and the modified DNA was suspended in 40 μl of Tris–ethylenediaminetetraacetic acid buffer (pH 8.0). An aliquot of 1 μl was used for methylation-specific PCR (MSP).

MSP was performed using primers as previously published (11,13,15,16) (Supplementary data, Table S1). For the *NR1I2* gene, although the combined bisulfite restriction analysis was performed in the previous study (10), MSP targeting the same region was used in this study. Using fully methylated and unmethylated DNA, the annealing temperature that specifically amplified only methylated or unmethylated DNA was determined. Also, a minimum number of PCR cycles to obtain visible bands was determined using the (un)methylated DNA, and four cycles were added for the analysis of primary NBLs (Supplementary data, Table S1).

Statistical Analysis

Survival time was defined as the time between initial diagnosis and death, or time between diagnosis and last contact if no event had occurred. Kaplan–Meier analysis and log-rank tests were conducted to compare survival between the groups defined by methylation status. HRs were estimated by the Cox

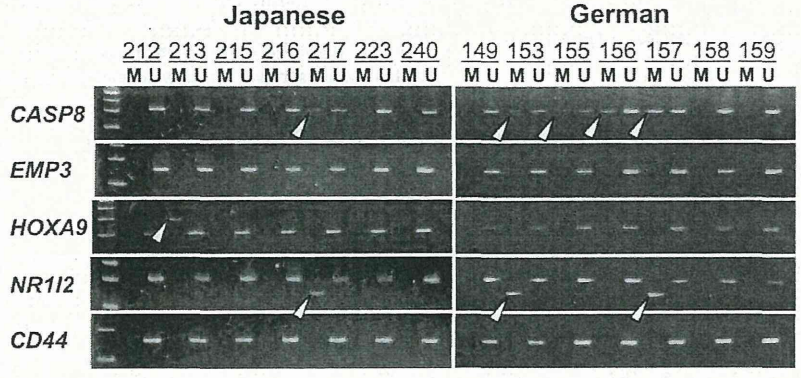

Figure 1. Methylation of promoter CpG islands (CGIs) of five individual genes (*CASP8*, *EMP3*, *HOXA9*, *NR1I2* and *CD44*) in Japanese and German neuroblastomas (NBLs). Representative results of methylation-specific PCR are shown. M and U, primers specific to methylated and unmethylated DNA, respectively. Arrowheads show the presence of methylated DNA molecules.

proportional hazard model. These statistical analyses were performed using the SPSS software, version 13.0 (SPSS Inc., Chicago, IL, USA).

RESULTS

Methylation of Individual Genes and their Prognostic Power Compared with CIMP

CASP8, *EMP3*, *HOXA9*, *NR1I2* and *CD44* were methylated in 26, 4, 27, 15 and 3, respectively, of the 140 Japanese NBLs, and in 30, 2, 2, 13 and 2, respectively, of the 152 German NBLs (representative results shown in Fig. 1). The prognostic power of methylation of the five genes was analyzed in Japanese and German NBLs, respectively (Fig. 2A and Table 1). In Japanese NBLs, only *CASP8* methylation had a significant association with poor survival (HR = 3.1; 95% CI = 1.5–6.4; $P = 0.002$). Regarding CIMP, defined by methylation of multiple genes and detected by methylation of the *PCDHB* gene family (2), it had a strong association with poor survival (HR = 22; 95% CI = 5.3–93; $P = 1.5 \times 10^{-5}$), and its prognostic power was stronger than that of *MYCN* amplification (HR = 9.5; 95% CI = 4.4–21; $P = 4.0 \times 10^{-9}$) (Fig. 2B). In the identical set of Japanese NBLs, a stronger prognostic power of CIMP than methylation of an individual gene was clearly shown.

In German NBLs, *CASP8* methylation was also associated with poor survival (HR = 4.8; 95% CI = 2.1–11; $P = 0.0002$) (Fig. 2A and Table 1). In addition, *HOXA9* and *NR1I2* methylation were associated with poor survival with an HR of 14 for *HOXA9* (95% CI = 3.1–62; $P = 0.0006$) and 4.2 for *NR1I2* (95% CI = 1.6–11; $P = 0.003$), respectively. Regarding CIMP and *MYCN*, as shown in our previous study (3), CIMP had a strong association with poor survival (HR = 9.5; 95% CI = 3.2–28; $P = 4.7 \times 10^{-5}$) and it was comparable to that of *MYCN* (HR = 12; 95% CI = 4.9–29; $P = 4.8 \times 10^{-8}$) (Fig. 2B). The stronger prognostic power of CIMP was consistently shown in the identical set of German NBLs.

Association Between CIMP and Methylation of Individual Genes

Among the five individual genes analyzed in this study, two genes (*CASP8* and *NR1I2*) were methylated at a significantly higher incidence in NBLs with CIMP (Fig. 3). In Japanese NBLs with and without CIMP, *CASP8* methylation was found in 24/67 and 2/73, respectively ($P = 5.0 \times 10^{-7}$). *NR1I2* methylation was found in 15/67 and 0/73, respectively ($P = 3.2 \times 10^{-5}$). Also in German NBLs with and without CIMP, *CASP8* methylation was found in 28/50 and 2/95, respectively ($P = 2.6 \times 10^{-14}$). *NR1I2* methylation was found in 11/50 and 1/95, respectively ($P = 1.4 \times 10^{-5}$). These results showed that CIMP was associated with methylation of multiple promoter CGIs, mainly *CASP8* and *NR1I2*.

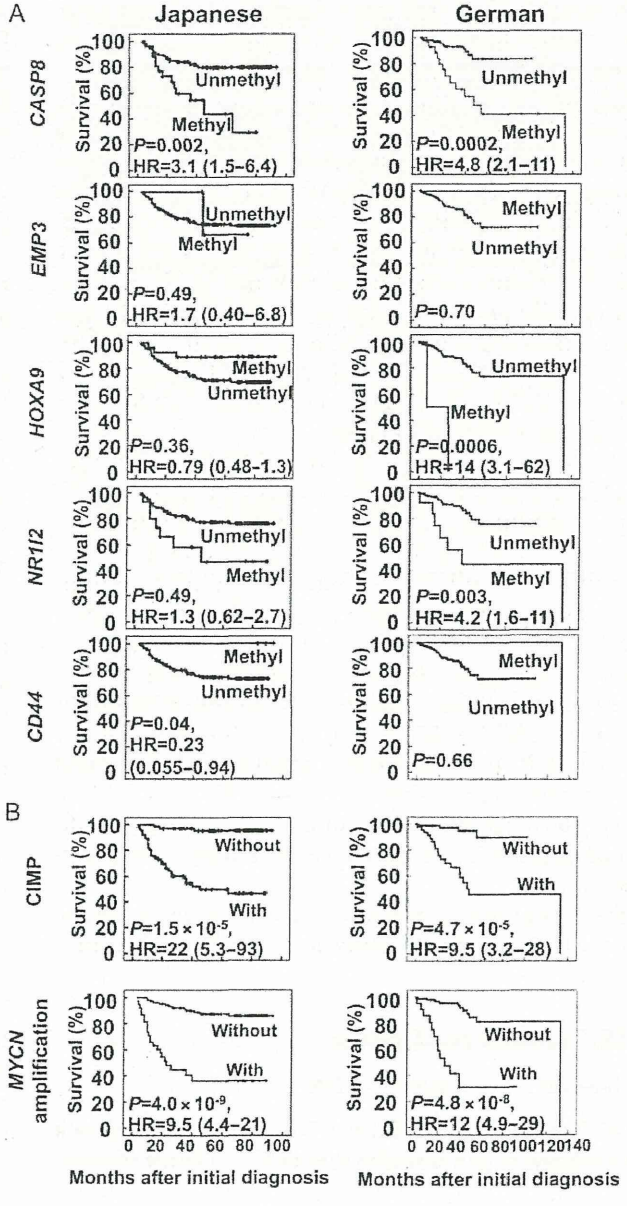

Figure 2. Prognostic power of (A) methylation of five individual genes (*CASP8*, *EMP3*, *HOXA9*, *NR1I2* and *CD44*), and (B) CpG island methylator phenotype (CIMP) and MYCN amplification in Japanese and German NBLs. Kaplan–Meier survival curves were drawn using the SPSS software. Among the five genes, only CASP8 methylation had a significant association with poor survival both in Japanese and German NBLs.

DISCUSSION

The stronger prognostic power of CIMP than methylation of individual genes was shown in this study. Also, the association between CIMP and methylation of multiple promoter CGIs was indicated. These results supported the idea that CIMP leads to a poor prognosis by induction of methylation of promoter CGIs of various tumor-suppressor genes with low incidences.

Table 1. Prognostic power of methylation of individual genes and CpG island methylator phenotype (CIMP)

Marker	Japanese ($n = 140$)				German ($n = 152$)			
	No. of NBLs with methylation or amplification	HR	95% CI for HR	*P* value	No. of NBLs with methylation or amplification	HR	95% CI for HR	*P* value
CASP8	26	3.1	1.5–6.4	0.002	30	4.8	2.1–11	0.0002
EMP3	4	1.7	0.4–6.8	0.49	2	NA	–	0.70
HOXA9	27	0.79	0.48–1.3	0.36	2	14	3.1–62	0.0006
NR1I2	15	1.3	0.62–2.7	0.49	13	4.2	1.6–11	0.003
CD44	3	0.23	0.055–0.94	0.04	2	NA	–	0.66
CIMP	67	22	5.3–93	1.5×10^{-5}	50	9.5	3.2–28	4.7×10^{-5}
MYCN amplification	38	9.5	4.4–21	4.0×10^{-9}	23	12	4.9–29	4.8×10^{-8}

NBL, neuroblastoma; HR, hazard ratio; CI, confidence interval; NA, not applicable.

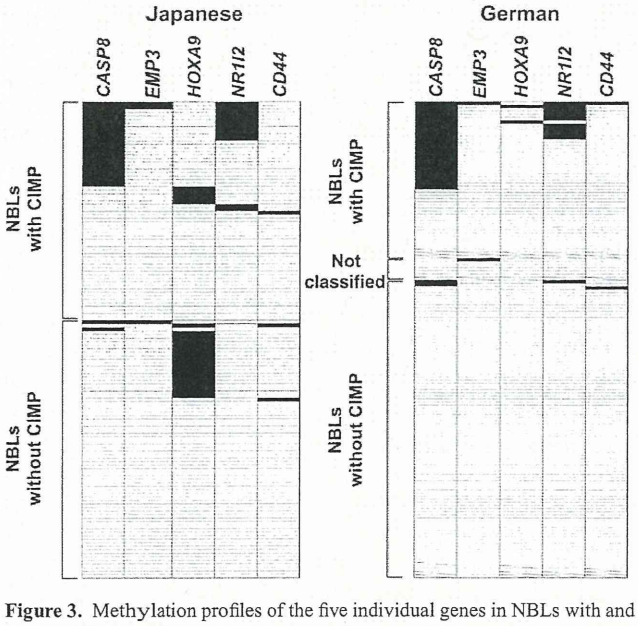

Figure 3. Methylation profiles of the five individual genes in NBLs with and without CIMP. Left panel, 140 Japanese NBLs; and right panel, 152 German NBLs. NBLs were classified by CIMP status determined as in our previous studies (2,3), and then aligned by methylation statuses of the five genes. In German NBLs, seven cases were not classified as NBLs with CIMP or without CIMP (3). The NBLs with CIMP tended to show methylation of multiple promoter CGIs. Closed box, methylated DNA detected; open box, only unmethylated DNA detected; and box with a slash; neither methylated nor unmethylated DNA detected, possibly due to low DNA quality.

Regarding the assessment of CIMP, besides the use of the *PCDHB* gene family, a combination of silenced genes has been proposed. Yang et al. (17) analyzed methylation of eight genes (*HIC-1*, *RASSF1A*, *BLU*, *DCR2*, *CASP8*, *TIG-1*, *HIN-1*, *TMS-1*), and identified that methylation of two and three genes had no effects on survival ($P = 0.719$ and 0.214, respectively), but methylation of ≥ 4 genes had a trend toward decreased survival ($P = 0.055$). Also, Lau et al. (18) identified that methylation of at least one of three genes (*FOLH1*, *MYOD1* and *THBS1*) was associated with event-free survival (HR = 2.2; 95% CI = 1.1–4.2; $P = 0.022$), and the association was stronger in methylation of all the three genes (HR = 4.5; 95% CI = 1.6–13; $P = 0.006$). These data support the model that CIMP leads to methylation of promoter CGIs of tumor-related genes with low incidences, which leads to poor survival.

Among the individual genes, *CASP8* and *RASSF1A* methylation have been repeatedly shown to be associated with poor survival (9,17,19–23). *CASP8* methylation was consistently associated with poor survival in the present study. By the analysis of methylation and survival data in our previous study (2), *RASSF1A* methylation was also revealed to be associated with poor survival in Japanese NBLs (HR = 4.2; 95% CI = 1.9–9.3; $P = 0.0005$). However, HRs of these genes were smaller than that of CIMP. These data indicated that these two genes play critical roles in a fraction of NBLs but not in the other NBLs. Indeed, a recent genome-wide methylation study revealed that methylation of numerous genes was associated with poor survival in NBLs (24).

In conclusion, the stronger prognostic power of CIMP than of methylation of individual genes was shown, and methylation silencing of various tumor-suppressor genes with low incidences was suggested to be involved in poor survival.

Supplementary data

Supplementary data are available at http://www.jjco.oxfordjournals.org.

Funding

This study was supported by Grants-in-Aid for the Third-Term Cancer Control Strategy Program from the Ministry of Health, Labour and Welfare, Japan and by the National Cancer Center Research and Development Fund, Japan.

Conflict of interest statement

None declared.

References

1. Maris JM, Hogarty MD, Bagatell R, Cohn SL. Neuroblastoma. *Lancet* 2007;369:2106–20.
2. Abe M, Ohira M, Kaneda A, et al. CpG island methylator phenotype is a strong determinant of poor prognosis in neuroblastomas. *Cancer Res* 2005;65:828–34.
3. Abe M, Westermann F, Nakagawara A, Takato T, Schwab M, Ushijima T. Marked and independent prognostic significance of the CpG island methylator phenotype in neuroblastomas. *Cancer Lett* 2007;247:253–8.
4. Banelli B, Brigati C, Di Vinci A, et al. A pyrosequencing assay for the quantitative methylation analysis of the PCDHB gene cluster, the major factor in neuroblastoma methylator phenotype. *Lab Invest* 2011;92:458–65.
5. Schwab M, Alitalo K, Klempnauer KH, et al. Amplified DNA with limited homology to myc cellular oncogene is shared by human neuroblastoma cell lines and a neuroblastoma tumour. *Nature* 1983;305:245–8.
6. Brodeur GM, Seeger RC, Schwab M, Varmus HE, Bishop JM. Amplification of N-myc in untreated human neuroblastomas correlates with advanced disease stage. *Science* 1984;224:1121–4.
7. Seeger RC, Brodeur GM, Sather H, et al. Association of multiple copies of the N-myc oncogene with rapid progression of neuroblastomas. *N Engl J Med* 1985;313:1111–6.
8. Ushijima T, Watanabe N, Okochi E, Kaneda A, Sugimura T, Miyamoto K. Fidelity of the methylation pattern and its variation in the genome. *Genome Res* 2003;13:868–74.
9. Grau E, Martinez F, Orellana C, et al. Hypermethylation of apoptotic genes as independent prognostic factor in neuroblastoma disease. *Mol Carcinog* 2011;50:153–62.
10. Misawa A, Inoue J, Sugino Y, et al. Methylation-associated silencing of the nuclear receptor 1I2 gene in advanced-type neuroblastomas, identified by bacterial artificial chromosome array-based methylated CpG island amplification. *Cancer Res* 2005;65:10233–42.
11. Alaminos M, Davalos V, Ropero S, et al. EMP3, a myelin-related gene located in the critical 19q13.3 region, is epigenetically silenced and exhibits features of a candidate tumor suppressor in glioma and neuroblastoma. *Cancer Res* 2005;65:2565–71.
12. Alaminos M, Davalos V, Cheung NK, Gerald WL, Esteller M. Clustering of gene hypermethylation associated with clinical risk groups in neuroblastoma. *J Natl Cancer Inst* 2004;96:1208–19.
13. Teitz T, Wei T, Valentine MB, et al. Caspase 8 is deleted or silenced preferentially in childhood neuroblastomas with amplification of MYCN. *Nat Med* 2000;6:529–35.
14. Kaneda A, Kaminishi M, Sugimura T, Ushijima T. Decreased expression of the seven ARP2/3 complex genes in human gastric cancers. *Cancer Lett* 2004;212:203–10.
15. Margetts CD, Morris M, Astuti D, et al. Evaluation of a functional epigenetic approach to identify promoter region methylation in phaeochromocytoma and neuroblastoma. *Endocr Relat Cancer* 2008;15:777–86.
16. Hoebeeck J, Michels E, Pattyn F, et al. Aberrant methylation of candidate tumor suppressor genes in neuroblastoma. *Cancer Lett* 2009;273:336–46.
17. Yang Q, Kiernan CM, Tian Y, et al. Methylation of CASP8, DCR2, and HIN-1 in neuroblastoma is associated with poor outcome. *Clin Cancer Res* 2007;13:3191–7.
18. Lau DT, Hesson LB, Norris MD, Marshall GM, Haber M, Ashton LJ. Prognostic significance of promoter DNA methylation in patients with childhood neuroblastoma. *Clin Cancer Res* 2012;18:5690–700.
19. Michalowski MB, de Fraipont F, Plantaz D, Michelland S, Combaret V, Favrot MC. Methylation of tumor-suppressor genes in neuroblastoma: the RASSF1A gene is almost always methylated in primary tumors. *Pediatr Blood Cancer* 2008;50:29–32.
20. Kamimatsuse A, Matsuura K, Moriya S, et al. Detection of CpG island hypermethylation of caspase-8 in neuroblastoma using an oligonucleotide array. *Pediatr Blood Cancer* 2009;52:777–83.
21. Yang Q, Zage P, Kagan D, et al. Association of epigenetic inactivation of RASSF1A with poor outcome in human neuroblastoma. *Clin Cancer Res* 2004;10:8493–500.
22. Banelli B, Gelvi I, Di Vinci A, et al. Distinct CpG methylation profiles characterize different clinical groups of neuroblastic tumors. *Oncogene* 2005;24:5619–28.
23. Banelli B, Bonassi S, Casciano I, et al. Outcome prediction and risk assessment by quantitative pyrosequencing methylation analysis of the SFN gene in advanced stage, high-risk, neuroblastic tumor patients. *Int J Cancer* 2010;126:656–68.
24. Buckley PG, Das S, Bryan K, et al. Genome-wide DNA methylation analysis of neuroblastic tumors reveals clinically relevant epigenetic events and large-scale epigenomic alterations localized to telomeric regions. *Int J Cancer* 2011;128:2296–305.